Raman studies of molecular-to-nonmolecular transitions in carbon dioxide at high pressures and temperatures

Amartya Sengupta[1] and Choong-Shik Yoo[1,2]
[1]*Institute for Shock Physics, Washington State University, Pullman, Washington 99164, USA*
[2]*Department of Chemistry, Washington State University, Pullman, Washington 99164, USA*
(Received 20 January 2009; revised manuscript received 7 July 2009; published 30 July 2009)

We have studied the molecular-to-nonmolecular phase transformations of carbon dioxide (CO_2) in laser-heated diamond-anvil cells by confocal micro-Raman spectroscopy. Our spatially resolved Raman data across the laser-heated area suggest that two distinct forms of extended phases, phase VIII and disordered phase, coexist with tetrahedrally coordinated phase V above 50 GPa but at somewhat lower temperatures. The existence of these phases are most evident from their characteristic Raman features, which include a strong mode at 1200 cm^{-1} for phase VIII and a broad peak at 900 cm^{-1} for disordered phase, both of which appear at substantially higher wave numbers than the ν_b(C-O-C) mode of phase V at ~800 cm^{-1}, around 50 GPa. Our Raman data further suggest that phase III is stable to at least 65 GPa at ambient temperatures and thus, emphasize that the stability field of *a*-carbonia, an amorphous extended phase, is only at elevated temperatures at pressures around 50 GPa or at room temperature above 65 GPa. This apparent extended stability of phase III may be due to strong kinetics associated with the molecular-to-nonmolecular transitions.

DOI: 10.1103/PhysRevB.80.014118 PACS number(s): 62.50.−p, 81.30.−t, 81.40.Vw, 78.30.−j

I. INTRODUCTION

Carbon dioxide (CO_2) is a simple molecule abundant in nature, which crystallizes into a typical molecular solid (CO_2-I, dry ice) at around 1 GPa. Its strong carbon-oxygen double bonds and relatively weak quadrupolar interactions make this molecular solid highly stable and chemically inert at relatively low pressures below 10 GPa. However, its structural stability and the nature of chemical bonding alter significantly at high pressures and temperatures, and CO_2 undergoes several interesting physical and chemical changes including the transitions to nonmolecular extended solids in three-dimensional covalently bonded network structures such as those found in SiO_2 and diamond.[1]

The phase diagram of CO_2 exhibits a large number of polymorphs that display highly diverse intermolecular and intramolecular interactions and crystal structures, as illustrated in Fig. 1. Previous high-pressure studies have shown the existence of at least eight solid phases of carbon dioxide below 50 GPa.[2–8] These include, molecular phases I ($Pa3$),[2] III ($Cmca$),[4] and VII (Ref. 7) ($Cmca$) at relatively low pressures below 10 GPa; associated phases II ($P4_2/mnm$) and IV ($Pbcn$) in an intermediate pressure region between 10–40 GPa (Ref. 3), and extended phases V ($P2_12_12_1$),[5] VI ($P4_2/mnm$),[6] and amorphous *a*-carbonia[8] above 40 GPa. These phases clearly indicate the pressure-induced enhancement of intermolecular interaction with increasing pressures, which leads to enhanced collective behaviors of molecules and eventually the formation of nonmolecular extended solids at higher pressures and high temperatures.

There appear to be striking crystallographic similarities between the high-pressure polymorphs of CO_2 and those of SiO_2 though this view has been challenged in recent times.[1] These include tridymite-type CO_2 phase V with fourfold coordinated carbon atoms,[9] stishovite-type CO_2 phase VI with sixfold coordinated carbon atoms,[6] and amorphous silica-type *a*-carbonia.[8]

There have been several uncertainties raised in recent years, regarding structural stabilities of the CO_2 phases both in theory and experiments.[10,11] *Ab initio* molecular dynamics (MD) simulations have suggested an interesting layered carbonate structure, namely, *m* chalcopyrite, in the stability field of phase V.[12] There is also evidence that phases II and IV might be strictly molecular and not associative in nature.[1,7] Most recent theoretical studies predict that the tetrahedral coordination in Carbon is stable to at least 900 GPa and some initial first-principles theory also predicts the stishovite-type structure of carbon dioxide to be stable only above 450 GPa,[13] which is in sharp contrast to the recent discovery of phase VI at such low pressures around 50–70

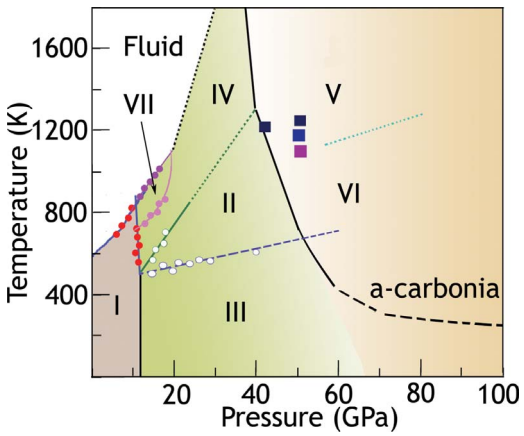

FIG. 1. (Color online) The phase/chemical transformation diagram of carbon dioxide. Solid lines indicate exact phase boundaries. The dashed lines between phases III and II (reproduced from Ref. 3) and between phase III and *a*-carbonia (reported in Refs. 8 and 20 and the present study) indicate a kinetic line. The broken melting line of phase IV has not been measured. The dotted lines between phase I and fluid CO_2 and between phases VII and IV have been reproduced from Ref. 7. The figure also indicates the experimental points of the present study in the vicinity of 1200 K and 50 GPa.

GPa.[6] Recent calculations[14] have also proposed that the observed phase VI may be a layered structure composed of a two-dimensional network of corner-sharing CO_4 tetrahedra instead of sixfolded. Recent theoretical calculations show that *a*-carbonia has mixed threefold and fourfold coordination in an equal proportion.[15]

The exact nature of the phase diagram is not well understood because of large lattice strains, phase metastabilities, and strong kinetics associated with the transitions. For example, the present phase diagram of CO_2 in Fig. 1 shows that the phase boundaries of phases I, III, II, and IV seem to meet at a same pressure-temperature (*P-T*) condition, 12 (1) GPa and 400 (5) K—which is quite unusual. In fact, the *Cmca* structure of phase III has been explained to be metastable at ambient temperatures with respect to phase II. The recently discovered phase VII also with a *Cmca* structure, near the melt supports this prediction.[7] Phase III on the other hand appears as a result of kinetically controlled martensitic transformation of phase I at relatively low temperatures and high pressures. Above 20 GPa, CO_2-III becomes quite unusual for a molecular solid, supporting huge pressure gradients (up to 100 GPa/mm). As a result, the exact nature of phase transition of phase III to amorphous CO_2 and/or *a*-carbonia is not well known even at ambient temperature. More significantly, the phase boundaries of phases V, VI, and *a*-carbonia are not well established. In fact, it is not very apparent if phase III is stable above 40 GPa or transforms to *a*-carbonia without elevating temperatures at pressures between 40–70 GPa. The stability field of phase V has been suggested to be as low as 640 K at 40–50 GPa,[16] where phase VI has recently been discovered.[6] It is considered that the metastability of phase V at low temperature may be responsible for the observation of phase V at such low temperatures.

Understanding the stability regions of such high *P-T* phases is important to understand the origin of carbonates in the deep interior of earth's mantle and also the formation of giant planets. In the present paper, we report a strong evidence for the coexistence of two distinct phases with phase V, formed by laser heating pure CO_2 between 40 and 60 GPa. We also compare the observed stability field of the phases with that of phase V and note higher stabilities of the discovered phases at low pressures.

II. EXPERIMENTAL DETAILS

It is important to note that many phases of CO_2 are metastable over a large *P-T* range well beyond their stability fields. For example, almost all CO_2 phases, except the apparent molecular phases I, III, and VII, can be quenched at room temperatures and at low pressures to around 10 GPa. Therefore, in order to evaluate the phase stability and boundary, it is important to maintain a consistent *P-T* path of experiments. Therefore, in this study we have used a membrane-diamond-anvil cell to compress (or heat) the sample isothermally (or isobarically) over a wide *P-T* range.

CO_2 samples were loaded in DACs from a liquid by condensing CO_2 gas to −35 °C and 15 atmospheres. Type IA diamond anvils were used with a culet size of 300 μm. A rhenium gasket was preindented to 40–50 μm thickness and a small hole of 127 μm was drilled using an electric-discharge microdrilling machine. A thin Pt foil (10 μm) was placed in the sample chamber to absorb the laser energy and heat the CO_2 sample using around 10–30 W laser power, depending on pressures. A few micrometer-sized ruby chips were scattered inside the cell for *in situ* pressure measurements.

In order to understand the structural variation/stability in the highly strained lattice, we have used a homebuilt confocal micro-Raman system in a back-scattering geometry using an Ar+ laser. The laser-heating system comprised of a single-mode Yb-fiber-coupled diode-pumped infrared laser with output power 100 W optimized at 1054 nm (YLM-100-SM-CS from IPG photonics). Long-working distance microscope objectives with a 20× magnification (NA=0.28, WD =30.5 mm and NA=0.4, WD=20 mm, both from Mitutoyo) were used to focus the Ar+ and IR lasers, respectively, to obtain the spot sizes of 5–8 and 12–15 μm, respectively. The heating of the sample was done indirectly via heating the Pt foil, creating a large temperature gradient (~100 K/μm) across the laser-heating spot. The Raman data was collected along the existing pressure gradient of the quenched sample (~100–200 GPa/mm). The pressure gradient was estimated by taking the Raman spectra at neighboring areas and looking at the peak shifts of the Raman bands as the probing laser spot was moved and comparing their values with the published literature. In this way, we can understand the structural variation over a highly strained lattice across the heated area—which has never been attempted in earlier studies.

III. RESULTS

CO_2 phase I transforms to phase III at around 10 GPa. Because of the martensitic nature, this transition is associated with a large pressure hysteresis and results in coexistence of the two phases over a large pressure range between 10–20 GPa. Having completed the transition at around 20 GPa, phase III develops an interesting texture evident for large lattice strains. The Raman spectrum of phase III consists of four Raman-active modes (A_g, B_{1g}, B_{2g}, and B_{3g} according to a factor group analysis[17]) which, because of the large lattice strain, are poorly resolved and appear as two broad bands above 20 GPa as shown in Fig. 2. Despite the broadness, the Raman spectra of CO_2 are characteristic to phase III over a large pressure range to 65 GPa—deep into the stability field for *a*-carbonia above 40 GPa as previously suggested.[8] Above 65 GPa, the Raman spectrum of CO_2 becomes featureless so is the x-ray diffraction pattern (not shown). This indicates that CO_2 becomes highly disordered. Nevertheless, it is important to note that the Raman and x-ray characteristics of CO_2 observed in the pressure range between 40–70 GPa are quite different from those previously reported for *a*-carbonia (see the top graph of Fig. 2).[8]

Above 40 GPa, laser-heating phase III transforms to an extended phase, CO_2-V. Figure 3 shows the Raman spectra of the hot spot after laser heating pure CO_2 between 40 and 50 GPa. Each of these spectra represents the results of laser heating a fresh sample of pure phase III which is important

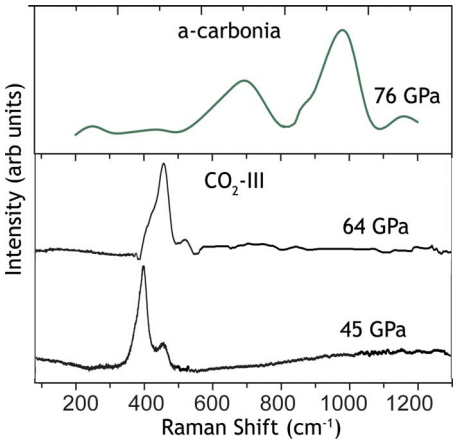

FIG. 2. (Color online) Raman spectrum of CO_2-III at 45 and 64 GPa. It is observed that even at 64 GPa, it is still a crystalline solid with relatively sharp vibrational modes in contrast with previous reports (Ref. 8). The top graph shows the analytically reproduced Raman spectrum of *a*-carbonia at 76 GPa from Ref. 8.

to characterize the stability field of phase V because of the metastability at ambient temperature. Optical pyrometry is used to measure the transition temperature, which is estimated to be 1200 °C (±30 °C) at the center of the hot spot.

It is apparent from Fig. 3 that the III-to-V transition requires the minimum pressure of 40 GPa. Yet, the Raman spectrum of phase V shows subtle differences depending on the transition pressure. For example, the bands at 1200 and 900 cm^{-1} become stronger with respect to the ν_b(C-O-C) mode at 800 cm^{-1} with increasing the transition pressure. The features between 250 and 500 cm^{-1} get substantially simplified at the higher transition pressures, as the relatively sharp feature at 470 cm^{-1} and a somewhat broad vibrational

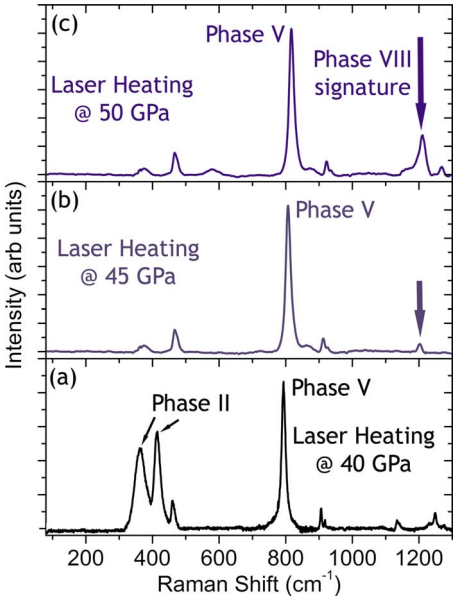

FIG. 3. (Color online) Raman spectra of the "hot" spot after laser heating at (a) 40, (b) 45, and (c) 50 GPa. An intense peak around 1200 cm^{-1} indicates the formation of a notable phase, phase VIII on laser heating above 50 GPa.

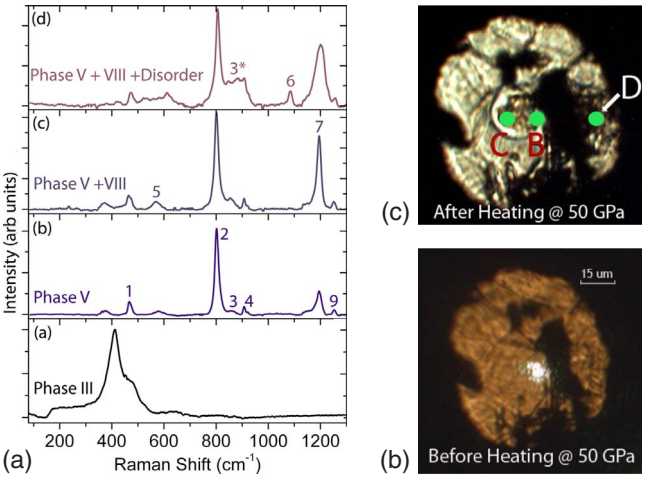

FIG. 4. (Color online) Raman spectrum (left panel) and *in situ* microphotographs of CO_2 at 50 GPa before heating (bottom right panel) and after heating (top right panel). The Raman spectra (b), (c), and (d) correspond to zones B, C, and D in the microphotograph of the top right panel which are phase V, phase VIII, and disordered phase, respectively. The Raman spectrum (a) was obtained from the marked area as shown in the microphotograph of the bottom right panel. The vibrational mode **8** is not visible at this pressure (see text and left panel of Fig. 6).

mode at 550 cm^{-1} dominate in this region. At or below 40 GPa, there is also an evidence of phase II formed together with phase V at the vicinity of laser-heating spot, which is evident from two most characteristic bands of phase II at 370 and 410 cm^{-1} [see Fig. 3(a)].[3,16]

Above 40 GPa, CO_2 exhibits a large pressure gradient, both before and after the laser heating. We measured the pressure gradient in untransformed phase III to be 150–200 GPa/mm whereas that in the laser-heated region to be about 100 GPa/mm. Despite such a large pressure difference, the Raman spectra obtained around the heated area are similar to each other below 50 GPa. However, when the sample is heated at or above 50 GPa, we observed striking differences in both Raman spectra and visual appearance across the laser-heated area, which we characterize into three different regions based on the Raman characteristics in Fig. 4: (i) the region B at the center of laser-heated spot, showing the 800 cm^{-1} band being dominant and characteristic to phase V [Fig. 4(b)], (ii) the region C near the center exhibiting a strong 1200 cm^{-1} band [Fig. 4(c)]—a feature not observed at this magnitude of intensity, and (iii) the region D far away from the laser-heated spot showing a broad band centered around 900 cm^{-1} and a new sharp feature at 1085 cm^{-1} [Fig. 4(d)]. Clearly, the observed Raman spectra in the region C and D suggest two distinct phases of CO_2, which we call phase VIII and disordered phase, respectively. Because the sample is heated conductively through Pt foil, the observed difference probably reflects the difference in the transition temperature. Then, it is likely that, as the temperature decreases, the stability of phases increases as phase V, to phase VIII, and to disordered phase. We would also like to point out that there is no evidence of any chemical reaction to have occurred between pure CO_2 and Pt in our experiments. Such reactions are known to be irreversible and no trace of any

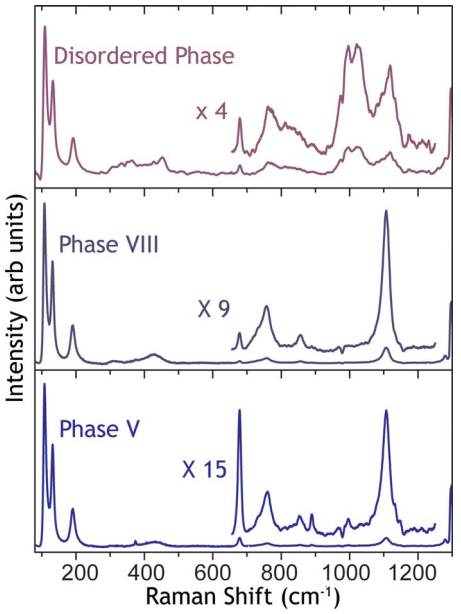

FIG. 5. (Color online) Raman spectra of the different zones at 4 GPa. Qualitative differences of the extended phases V, VI, and VIII, and disordered are evident from the above graphs (for further details, see text).

chemically reacted material was found after complete unloading and reloading the same sample. The Raman spectrum of the reloaded sample (not shown) at 5 GPa represented the well-known CO_2-I.

Phase VIII and disordered phase exhibit several characteristic Raman features that have not been observed previously in any other CO_2 phases. The latter phase, for example, is mostly evident from a broad peak **3*** centered around 880 cm^{-1} and a relatively sharp peak **6** at 1085 cm^{-1} in Fig. 4(d). Phase VIII on the other hand, is evident from an intense sharp peak **7** at ~1200 cm^{-1} in Fig. 4(c). Note that a similar peak also appears in phase V—but only with a substantially reduced intensity particularly when produced below 50 GPa [Figs. 3(a) and 3(b)]. In contrast, at or above 50 GPa, this peak is appreciably intense at the center of hot spot [Fig. 4(b)] and is as intense as the characteristic ν_b(C-O-C) peak **2** of phase V at the vicinity of hot spot [Fig. 4(c)]. This result indicates that phase VIII is favorable at higher pressures and lower temperatures than phase V. In addition, we also observe a new peak at ~570 cm^{-1} (peak **5**), not observed in the previous experiments. A previous theoretical calculation of phase V has, however, predicted similar vibrational features (especially regarding the 1200 cm^{-1} band, peak **7**) for a β-cristobalite-type CO_2 structure.[18] Therefore, it is possible that the structure of phase VIII is related to that of β cristobalite.

These extended phases, including phase VIII, disordered, and phase V are metastable at room temperatures and at relatively low pressures but all eventually transform back to phase I below 10 GPa. Important to note, however, is the significant differences in how they transform back to phase I, as highlighted in Fig. 5. Around 3 GPa, for example, the peak intensities of the 1200 cm^{-1} band in phase VIII and the 900 cm^{-1} band in disordered phase are much stronger with respect to that of the 800 cm^{-1} band in phase V.

The pressure dependence of Raman spectra also reveals the difference among the extended phases V, VIII, and disordered, as summarized in Fig. 6. The Raman spectra obtained of phase V and their pressure dependences are, in general, consistent with the previously reported results,[5,16] with the exception of peak **8** (Raman spectra, not shown). One previous study[16] reported the presence of asymmetry on the lower-frequency side of peak **2**, which is now resolved as

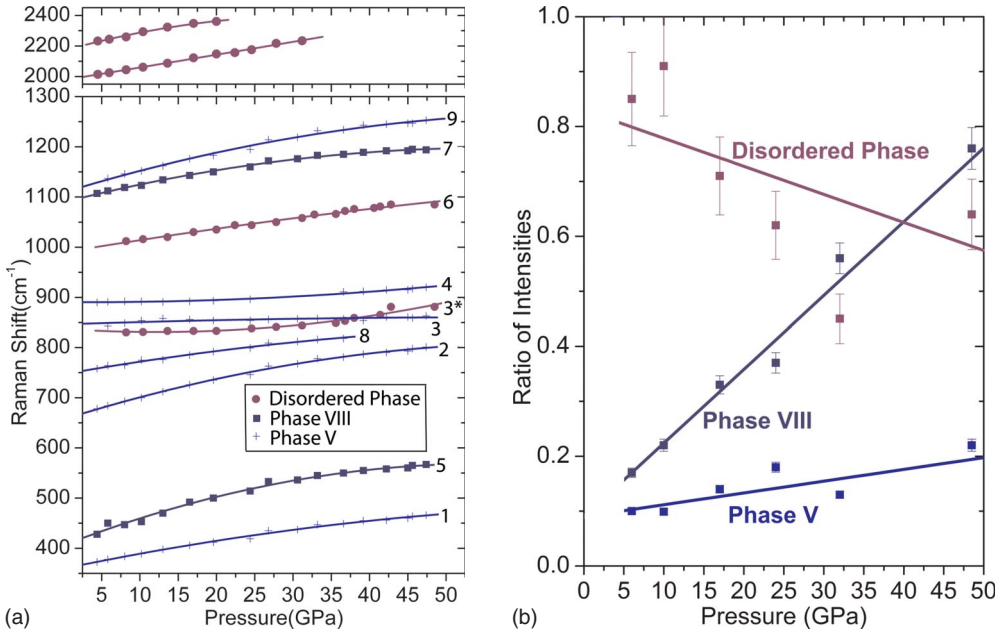

FIG. 6. (Color online) (Left) Frequency dependence of the vibrational modes of the different phases. The pressure error bars range between ±1 and ±2 GPa. For numbering details, see text. (Right) Intensity ratios of the characteristic peak of phase VIII (peak **7**) and the disordered phase (peak **3***) as the pressure is released.

peak **8** from 36 GPa all the way down to 4 GPa as shown in Fig. 6 (left panel).

Important to note is that some peaks previously assigned for phase V, including peaks **5** and **7**, should be assigned to the vibrational modes of phase VIII. Interestingly, both peaks of phase VIII exhibit different pressure dependences, that is, a strong pressure shift of peak **5** while a linear pressure dependence of peak **7**. This indicates that the nature of the chemical bonding, that is, involved with the respective vibrational modes is somewhat different and one is stronger than the other. Also, the pressure dependence of peak **2** (characteristic of phase V) and peak **7** (characteristic of phase VIII) are substantially different which is a further evidence for the latter being the signature of a distinct phase.

In the disordered phase zone, peak **3*** has a very weak dependence on pressure while peak **6** has an almost linear dependence with pressure. This means that the origin of the peaks of the disordered phase is very different. Also, peak **6** which is relatively sharp around 50 GPa gradually becomes broader as the pressure is released and is not detectable below 8 GPa. As we unload the pressure below 30 GPa, we also observed the appearance of two new relatively broad bands at around 2200 and 2400 cm^{-1} with a linear pressure dependence (8.2 cm^{-1}/GPa), both of which can be traced all the way down to 4 GPa.

IV. DISCUSSIONS

A characteristic behavior of CO_2 at high pressures is its large lattice strain and phase metastability. Large strain seems to reflect its pressure-enhanced intermolecular interaction, leading to highly "unusual" molecular solid phase III above 20 GPa and eventual transformations to extended solids at higher pressures. Nevertheless, the present Raman data in Fig. 2 clearly indicates the existence of phase III at pressures of at least 65 GPa, although the lattice is highly strained and the structure may be distorted (or disordered). It is different from *a*-carbonia. The lack of the transformation of phase III to *a*-carbonia may then be explained in terms of a large kinetic barrier associated with the transition, as seen in other molecular-to-nonmolecular transitions including nitrogen.[19] In fact, it is the very reason why phase III is not converted to phase II—the phase predicted to be stable between 20 and 40 GPa and why *a*-carbonia has never been produced without heating phase III in the pressure range between 50–70 GPa. A recent study also shows that phase III transforms to *a*-carbonia only above 65 GPa at ambient temperature.[20]

The present data provide further constraints for the stability field of phase V, that is, different from a previous study suggesting it as low as 640 K between 40–50 GPa.[16] In fact, the present study indicates phase VIII and/or disordered phase (see Fig. 4) to exist between phase V and phase III. Also, recall that phase VI and *a*-carbonia exist in this intermediate temperature range. We attribute this difference to the metastability of phase V that makes difficult to determine the exact transition temperature based on the Raman spectra in the previous study.[16]

The present study offers two additional forms of extended CO_2 solids: phase VIII and disordered phase, both of which were stabilized above 50 GPa. The disordered phase is produced in the region relatively far away from the laser-heating spot at 50 GPa and its Raman spectrum is different from that of *a*-carbonia because if we extrapolate our data to 76 GPa, for the disorder band **3***, the frequency shifts are at least 100 cm^{-1} off from previous literature.[8] In addition to the above, the *a*-Carbonia band around 1900 cm^{-1} at 60 GPa (Ref. 15) does not translate to the two bands that we start observing from about 35 GPa. The Raman bands are about 100–150 cm^{-1} off from the phase VI disorder.[6] Furthermore, *a*-carbonia was synthesized at ambient temperatures at much higher pressures in earlier studies[20] and there is no evidence that it has been completely synthesized at pressures around 50 GPa.[8,15]

Phase VIII is a distinct phase, most evident from the characteristic Raman band at 1200 cm^{-1} [peak **7** in Fig. 4(c)] and not been reported in the earlier studies.[5,16,21] From the series of laser-heating experiments performed between 40 and 50 GPa, it is evident that the stability field of phase VIII is at higher pressures and lower temperatures with respect to phase V. The diminishingly weak intensity of peak **7** below 50 GPa in Fig. 3 supports this conclusion.

The stability fields of phase VIII and disordered phase are entirely different from phase V, as inferred by the intensities of their most characteristic peaks **7, 3,** and **2** in Fig. 4. Figure 6 (right panel) illustrates the pressure-dependent intensity changes in peak **7** in phase VIII and peak 3 in disordered phase intensities with respect to that of peak **2** in phase V, as plotted by the ratios of peak **2** at 50 GPa, I_{800}). Note that as the pressure decreases the ratio for phase VIII gradually falls off, indicating that phase VIII might be less stable than phase V at lower pressures while the disorder gradually increases. Since most of the previous reports including the current work have observed traces of peak **2**, when CO_2-III was laser heated around 40 GPa and above, it appears that the synthesis of phase VIII is intricately linked to that of phase V. It may well possess a similar structure with a common structural building block such as corner-sharing CO_4 tetrahedra, which include the β-cristoballite-type structure, as mentioned above and predicted in previous MD simulations.[18] However, the experimental validation of this conjecture clearly requires further studies to determine the crystal structures.

V. CONCLUSIONS

In summary, we have presented the evidence for two extended phases of carbon dioxide by performing Raman spectroscopy measurements—phase VIII and disordered phase, both synthesized by laser heating pure CO_2-III at or above 50 GPa and at lower temperatures than that required for phase V. Similar runs at lower pressures between 40 and 45 GPa did not yield the newly discovered phases, suggesting the stability fields of the phases above 50 GPa. The present study also asserts that the stability field of phase III is well above 50 GPa and transformation to *a*-carbonia should be at higher temperatures around 50 GPa or at significantly higher pressures.

ACKNOWLEDGMENTS

We appreciate Kurt Zimmerman at WSU for his experimental assistance. The work has been supported by NSF-DMR (Grant No. 0854618), DTRA (Grant No. HDTRA 1–09–1–001–41), and DOE-NNSA (Grant No. DE-F603-97SF21388).

[1] M. Santoro and F. A. Gorelli, Chem. Soc. Rev. **35**, 918 (2006).
[2] J. W. Schmidt and W. B. Daniels, J. Chem. Phys. **73**, 4848 (1980).
[3] V. Iota and C. S. Yoo, Phys. Rev. Lett. **86**, 5922 (2001).
[4] R. C. Hanson, J. Phys. Chem. **89**, 4499 (1985).
[5] V. Iota, C. S. Yoo, and H. Cynn, Science **283**, 1510 (1999).
[6] V. Iota, C. S. Yoo, J.-H. Klepeis, Z. Jenei, W. Evans, and H. Cynn, Nature Mater. **6**, 34 (2007).
[7] V. M. Giordano and F. Datchi, EPL **77**, 46002 (2007).
[8] M. Santoro, F. A. Gorelli, R. Bini, G. Ruocco, S. Scandolo, and W. A. Crichton, Nature (London) **441**, 857 (2006).
[9] C. S. Yoo, H. Cynn, F. Gygi, G. Galli, V. Iota, M. Nicol, S. Carlson, D. Hausermann, and C. Mailhiot, Phys. Rev. Lett. **83**, 5527 (1999).
[10] M. S. Lee, J. A. Montoya, and S. Scandolo, Phys. Rev. B **79**, 144102 (2009).
[11] J. Sun, D. D. Klug, R. Mortonak, J. A. Montoya, M. S. Lee, S. Scandolo, and E. Tosatti, Proc. Natl. Acad. Sci. U.S.A. **106**, 6077 (2009).
[12] S. Serra, C. Cavazzoni, G. L. Chiarotti, S. Scandolo, and E. Tosatti, Science **284**, 788 (1999).
[13] B. Holm, R. Ahuja, A. Belonoshko, and B. Johansson, Phys. Rev. Lett. **85**, 1258 (2000).
[14] A. Togo, F. Oba, and I. Tanaka, Phys. Rev. B **77**, 184101 (2008).
[15] J. A. Montoya, R. Rousseau, M. Santoro, F. Gorelli, and S. Scandolo, Phys. Rev. Lett. **100**, 163002 (2008).
[16] M. Santoro, J. F. Lin, H. K. Mao, and R. J. Hemley, J. Chem. Phys. **121**, 2780 (2004).
[17] F. A. Cotton, *Chemical Applications of Group Theory* (John Wiley and Sons, New York, 1990).
[18] J. Dong, J. K. Tomfohr, and O. F. Sankey, Phys. Rev. B **61**, 5967 (2000).
[19] C. Mailhiot, L. H. Yang, and A. K. McMahan, Phys. Rev. B **46**, 14419 (1992).
[20] T. Kume, Y. Ohya, M. Nagata, S. Sasaki, and H. Shumizu, J. Appl. Phys. **102**, 053501 (2007).
[21] V. Iota and C. S. Yoo, Phys. Status Solidi B **223**, 427 (2001).